THREE-PHASE CAPILLARY PRESSURE MEASUREMENTS IN CENTRIFUGE AT RESERVOIR CONDITIONS

G. A. Virnovsky, K.O. Vatne, J.E. Iversen, RF-Rogaland Research, and C. Signy, ENSG-RF.

This paper was prepared for presentation at the International Symposium of the Society of Core Analysts held in Abu Dhabi, UAE, 5-9 October, 2004

ABSTRACT

The paper describes an experimental setup, interpretation procedure and analysis of a 3-phase centrifuge test at elevated pressures and temperatures. The interpretation procedure used is a generalization of the classical procedure commonly used for 2-phase flow. It takes into account that all three fluids present in the system, oil, water and gas, are mobile, and it requires that compressibility of the fluids be negligibly small.

A number of high-pressure centrifuge tests have been performed to study the effect of gravity drainage by gas followed by waterflooding on the efficiency of the oil recovery from Berea sandstone. Initially the core samples are saturated with oil and water at different proportions. The elevated pressure is essential to approach the realistic interfacial tensions between all the three phases present in the core, and also to reduce the compressibility of the gas phase. In the tests the initial water saturation varied. We report the results of the high-pressure tests and compare them with the similar tests performed at room conditions. The comparison shows a noticeable difference, which indicates the importance of the high-pressure centrifuge tests for accurate evaluation of the oil recovery at three-phase flow conditions.

INTRODUCTION

Three phase flow properties are important for correct modeling and prediction of such IOR processes like WAG and depletion after waterflooding. One of the most efficient tools in the special core analysis arsenal is centrifuge. Though centrifuge technique is widely used, the centrifuge tests for capillary pressure and relative permeability are normally not available at reservoir conditions. These conditions are important in 2-phase flow, but in three phase experiments they are believed to become crucial.

Generally, the elevated pressures and temperatures enable us to use live fluids, and hence to reproduce (1) realistic wettability conditions in the core, (2) realistic interfacial tensions, and hence spreading conditions, and also (3) to obtain negligible compressibility of the gas phase. In this paper we are only addressing the last 2 issues, i.e. the wettability issue is not addressed, since experiments were performed with model fluids.

To the best of our knowledge, the only attempt to experimentally measure three-phase capillary pressure with all phases mobile was made by Kalaydjian et al[1]. By using the

porous plate technique a gas drainage capillary pressure was measured in presence of water (both mobile and immobile), and a water imbibition capillary pressure was measured in presence of initial gas. It was concluded that the imbibition capillary pressure between gas and oil depends on both water and gas saturation.

A number of papers report the results of measurement of three-phase capillary pressure by the porous plate method when one of the three phases is immobile [2-4].

Since the classical paper by Hassler and Brunner[5] the centrifuge method has become a standard technique to measure capillary pressure and residual oil saturation for a two-phase displacement processes, i.e., gas drainage of oil, or forced imbibition of water into an oil saturated sample. An extensive study of three-phase capillary pressure measurements by centrifuge assuming that one of the phases is immobile is reported in Ref. [6]. A generalization of Hassler-Brunner method to three-phase experiments with all phases mobile was presented in Ref. [7].

INTERPRETATION OF 3-PHASE P_C MEASUREMENTS IN CENTRIFUGE

Assuming all three fluids to be incompressible, the distribution of the three saturations at static conditions (i.e. at zero velocity) in the field of centrifugal force is considered similarly to the two-phase case [7]. After some manipulations, one derives a set of two linear integral equations for the 2 unknown functions, i.e., 2 saturations as functions of 2 capillary pressures. As it is noticed in Ref. [7], at static conditions these capillary pressures are not independent, there exists an interrelation between them (if all the phases are mobile):

$$\frac{P_{cgo}(r)}{P_{cow}(r)} = \frac{\Delta\rho_{go}}{\Delta\rho_{ow}} = \gamma \qquad (1)$$

As a consequence of the interrelation (1), the system of the integral equations splits into 2 independent integral equations, which can be solved separately. These equations are as follows:

$$\overline{S}_w(P_{cwo}^{-1}) = 0.5(1+f)\int_0^{P_{cwo}^{-1}} v_w(z)\frac{dz}{\sqrt{1-\frac{z}{P_{cwo}^{-1}}(1-f^2)}} \qquad (2)$$

$$\overline{S}_g(P_{cgo}^{-1}) = 0.5(1+f)\int_0^{P_{cgo}^{-1}} v_g(z)\frac{dz}{\sqrt{1-\frac{z}{P_{cgo}^{-1}}(1-f^2)}}$$

with

$$v_w(P_{cwo}) = S_w(P_{cwo}, \gamma P_{cwo}), v_g(P_{cgo}) = S_g(P_{cgo}/\gamma, P_{cgo}) \quad (3)$$

$$P_{cij}{}^{1}(\omega) = \frac{1}{2}(r_1^2 - r_2^2)\Delta\rho_{ij}\omega^2$$

This analysis enables us to conclude that the interpretation of the three-phase centrifuge test can be performed using the same software as commonly used for the conventional, i.e. 2-phase centrifuge test.

In this work, we used the commercial package developed by *D&B Ruth Enterprises Inc*. called *PORCAP*. This program is capable of analysing the data according to different procedures but we chose Forbes Alpha method because this method seemed the best with respect t to reproduction of both residual saturations and cumulative production.

For the same reasons we chose the Rajan smoothed differencing method among the different options of numerical differentiation available in this software (Backward differencing, Central differencing, Forward differencing, Least squares differencing, Rajan smoothed differencing, 3rd order polynomial smoothed differencing).

EXPERIMENTAL ARRANGEMENT

The centrifuge coreholder schematic is shown in Figure 1. With the core holders used in these tests the maximum speed of rotation in the centrifuge is 2800 RPM. The maximum temperature is 120 ^{o}C. The core holders are designed for maximum sleeve pressure of 8000 psi, and maximum pore pressure of 5000 psi. The fluid collection section is a sapphire tube allowing visual reading of volume (i.e. reading the positions of the menisci). Core diameter is 1.5", maximum core length is 4.8 cm. The inlet and the outlet radii of the core mounted in the centrifuge core holder are given in Table 1. A stroboscope synchronized with the rotation of the centrifuge axis is used to facilitate the readings.

Four Berea core samples with similar properties (porosity and gas absolute permeability) were chosen for the test. The core properties are given in Table 2.

The brine composition is simulated sea water known to be compatible with the Berea. The gas and oil is an equilibrated combination of methane (C1) and n-heptane (C7). This system is chosen because its properties are described in the literature[8]. Heptane and methane are equilibrated in a piston cell at the temperature and pressure to be applied in the test. To load fluids in the fluid collector section of the core holder, this section is initially pressurized with the methane, and subsequently, the liquids are pumped in. Pertinent fluid properties are given in Table 5, Table 6 and Table 7.

All tests are made at 71.1^{o}C, and 2 pore pressures: 50 bar and 1 bar. For the tests at 50 bar, the procedure includes gas drainage and subsequent forced water imbibition, for the test at 1 bar, the water imbibition is excluded.

The selected 4 samples are initially saturated completely with the brine by (i) evacuating the dry core, (ii) injecting water to a reference pressure (20 bar), and (iii) flooding the

core with brine towards a back-pressure (8 bar). The samples are then subjected to primary drainage by oil in centrifuge to 4 different initial water saturations.

Gas Drainage. The collector and the bypass tubing are filled with the gas, with a small reference volume of water at the bottom of the collector section. The centrifuge is then run with the core holders in the drainage position at monotonously increasing speeds. The minimum speed is 400 RPM is chosen as it is difficult to read the meniscus positions at lower speeds. Maximum speed is chosen 2500 RPM.

Water Imbibition. Collector section is filled with brine. With the core holders in the imbibition position, the produced gas and oil is visually read out at equilibrium at each of a set of monotonously increasing speeds. Minimum and maximum speeds are chosen with the same rationale as for the gas drainage.

Fluid Volumes Control. After completing the final step in centrifuge, the saturations in the core are determined by blow-down and vacuum distillation. Produced liquid volumes are determined from weighting.

EXPERIMENTAL RESULTS

Saturation Trajectories. The initial average saturation in the cores is 100% water. The initial and the average saturations observed after each displacement step are displayed in Table 4 and Table 3, and also shown in Figure 3 and Figure 2. The oil saturation after gas drainage for core 5 was significantly higher in both experiments, at 50 bar and 1 bar, compared with the three other core samples. The reason for this was not investigated any further, but we believe it was related to differences between the core samples.

The saturation trajectories are shown in Figure 4 and Figure 5 for the gas drainage step. The subsequent water imbibition is not shown on the plot at 50 bar since there was almost no oil production observed and hence these trajectories are all straight lines parallel to the line S_o=0. One can easily observe from the plot and form the tables that the residual oil at 50 bars is very low. It is significantly lower than its counterpart at atmospheric pressure (except for the sample 5). This is, obviously, due to the difference in the interfacial tensions between gas and oil, which causes differences in the spreading coefficient values (see Table 7). The effect of spreading was reported to be crucial in three-phase gas drainage process by Vizika and Lombard[9]. In water-wet rock, the experimental results[9] showed higher oil recovery for positive spreading coefficient than when the spreading coefficient is negative. In our case all cores are water wet, and higher pore pressure (50 bar) corresponds to a somewhat higher spreading coefficient, so the observed difference in the residual oil is in line with the conclusions in Ref. [9].

Capillary Pressure Functions.

Generally, the two three-phase capillary pressure functions are dependent on 2 saturations, and can be represented as surfaces over the saturation domain Δ.

$$\Delta: \quad 0 \le S_w \le 1, \quad 0 \le S_g \le 1, \quad S_w + S_g \le 1 \qquad (4)$$

We, however, do not have sufficient data for this representation since the interpreted saturation points only cover a small part of the saturation domain Δ, namely, the area of small oil saturations; see Figure 4 and Figure 5. As one clearly observes from the plots, the interpreted saturation trajectories are mainly parallel to the line $S_w + S_g = 1$, which means that the oil saturation is constant along each trajectory (for high enough drainage pressure).

Capillary pressure curves are depicted in Figure 6 and Figure 7 for the gas drainage process for both 50 bar and 1 bar pore pressures, and in Figure 9 for the subsequent water imbibition process at 50 bar.

Note that in Figure 6 there is a significant difference between the corresponding curves measured at two different pressures. To test the assumption that the capillary pressure curves are linearly scaled with the gas-oil interfacial tension the set of gas-oil capillary pressure curves at 50 bar and its counterpart at 1 bar in Figure 8 are drawn in different scales. The scales are chosen such that the corresponding P_c curves should match if the assumption holds.

As one observes from Figure 6 and Figure 8 this assumption is not always fulfilled in our experiments. Except for the core 6 a significant deviation between the corresponding curves persists also in the rescaled view (though it became somewhat smaller).

Similarly, as observed from Figure 7, the corresponding oil-water capillary pressure curves do not match, though the interfacial tension between water at oil does not significantly change in the pressure interval of 1-50 bar.

We conclude therefore that simple scaling of capillary pressure with respect to the interfacial tension does not apply in three-phase gas drainage, which means that the *SCAL* program, in particular, the residual oil and capillary pressure measurements have to be performed at representative reservoir conditions.

Capillary pressure curves for water imbibition after gas drainage are presented in Figure 9. The centrifuging was started right after the completion of gas drainage, and hence the first point on the curves includes also spontaneous imbibition of water. Normally, in a two-phase water-gas flow one would expect around 60% of gas recovery due to spontaneous imbibition of water in water-wet Berea sandstone[10], which complies with our results. The remaining gas (and eventually oil) is partly displaced during forced water imbibition process. The maximal water saturations observed after forced water imbibition are roughly 70% in 3 samples and roughly 90% in one sample, see Table 4.

DISCUSSION AND CONCLUSIONS

A set of three-phase displacements has been performed in centrifuge at elevated temperature and pore pressure. We have reported the results of these centrifuge tests and compared it to a similar test performed at ambient conditions. This comparison shows a noticeable difference. The observed difference is both in residual saturations and in capillary pressures. We found it impossible to rescale the capillary pressure curves from the ambient test using the reduced value of the gas-oil interfacial tension in order to match their counterparts at elevated pressure.

The interpretation of three-phase centrifuge measurements is performed taking into account that all the fluids are mobile. An interpretation procedure to obtain three phase capillary pressures as function of 2 saturations derived earlier has been utilized.

The obtained data set covers only a small part of the saturation domain close to the residual oil saturation. More experimental data are required to derive conclusions about the behaviour of three-phase capillary pressure as function of two saturations in the saturation domain.

NOMENCLATURE

$f = \frac{r_1}{r_2}$ radius ratio

L_c core length

p_i individual phase pressure in the *i*-th phase, *i=w, o, g*

P_{cij} capillary pressure, $P_{cij} = p_i - p_j$

$P_{cij}^{\ 1} = P_{cij}(r_1), P_{cij}^{\ 2} = P_{cij}(r_2)$

r radius

r_1, r_2 radii of the inlet and the outlet boundary

S_i saturation of the *i*-th phase

$\overline{S}_i$ average saturation of the *i*-th phase

ρ_i density of the *i*-th phase

$\Delta\rho_{ij}$ density difference, $\Delta\rho_{ij} = \rho_i - \rho_j$

γ density contrast ratio defined in equation (1)

σ interfacial tension

ω angular velocity

REFERENCES

1. Kalaydjian F: Performance and analysis of three-phase capillary pressure curves for drainage and imbibition in porous media, in *SPE ATCE* (vol Reservoir Engineering), Washington DC, 1992, SPE 24878, pp 135-149
2. Dumore JM, Schools RS: Drainage capillary pressure functions and the influence of connate water. *SPE Journal (Oct 1974)*:437-444., 1974, SPE 4096
3. Longeron D, Kalaydjian F, Bardon C, Desremaux LM: Gas -oil capillary pressure: measurements at reservoir conditions and effect on gas-gravity drainage, in *SPE ATCE*, New Orleans, LA, USA, 1994, SPE 28612
4. Longeron D, Kalaydjian F, Bardon C: Gas -oil capillary pressure measurements at reservoir conditions: effect of interfacial tension and connate water saturation, in *7th European IOR Symposium*, Moscow, Russia, 1993, p 466
5. Hassler GL, Brunner E: Measurement of capillary pressure in small core samples. *Trans. AIME* 160:114-123, 1945
6. Toskey ED: Effect of the presence of a third phase on capillary pressure of consolidated sandstone by the centrifuge method, in, Fairbanks, USA, U. of Alaska, 1990, p 88
7. Virnovsky GA, Iversen JE: Measurement of three-phase capillary pressure by centrifuge, in *European IOR Symposium*, Brighton, UK., 1999
8. Bardon C, Longeron D: Influence of very low Interfacial tensions on relative permeability. *SPE Journal*, 1980, SPE 7609
9. Vizika O, Lombard J-M: Wettability and spreading: two key parameters in oil recovery with three phase gravity drainage. *SPE Reservoir Engineering*:54-60, 1996, SPE 28613
10. Li K, Firoozabadi A: Experimental study of wettability alteration to preferential gas-wetting in porous media and its effects. *SPE Reservoir Evaluation & Engineering* 3, 2000

ACKNOWLEDGEMENT

The results presented in the paper are obtained within a project on three-phase capillary pressure funded by ConocoPhillips. The financial support and permission to publish are gratefully acknowledged.

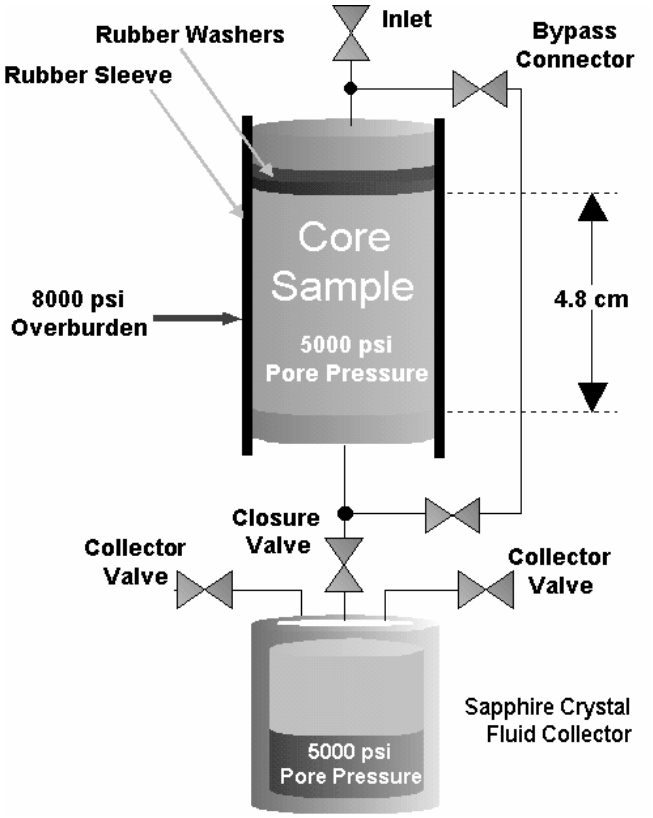

Figure 1: Centrifuge core holder schematic.

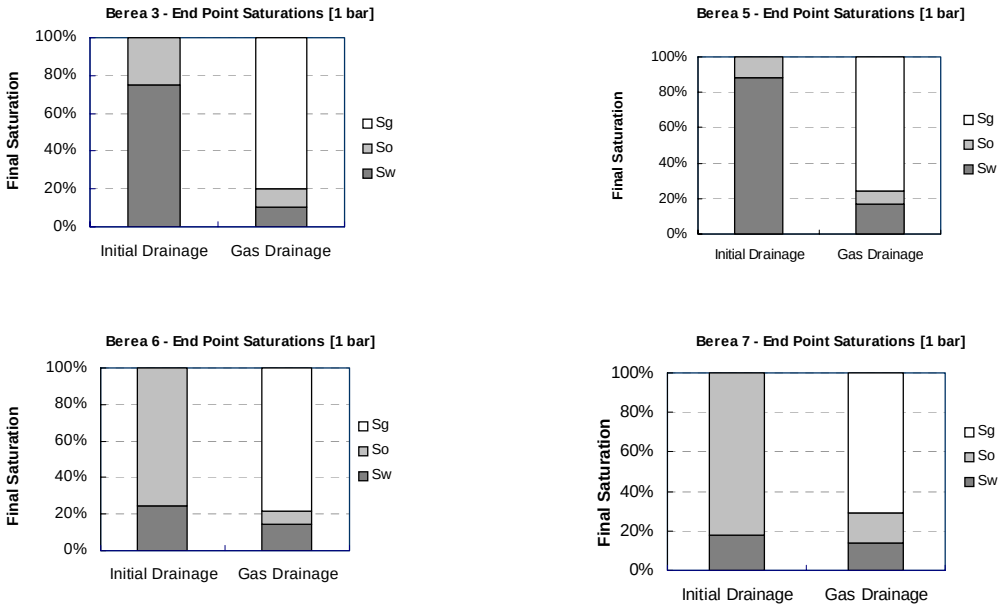

Figure 2: Residual saturations for the tests at 1 bar.

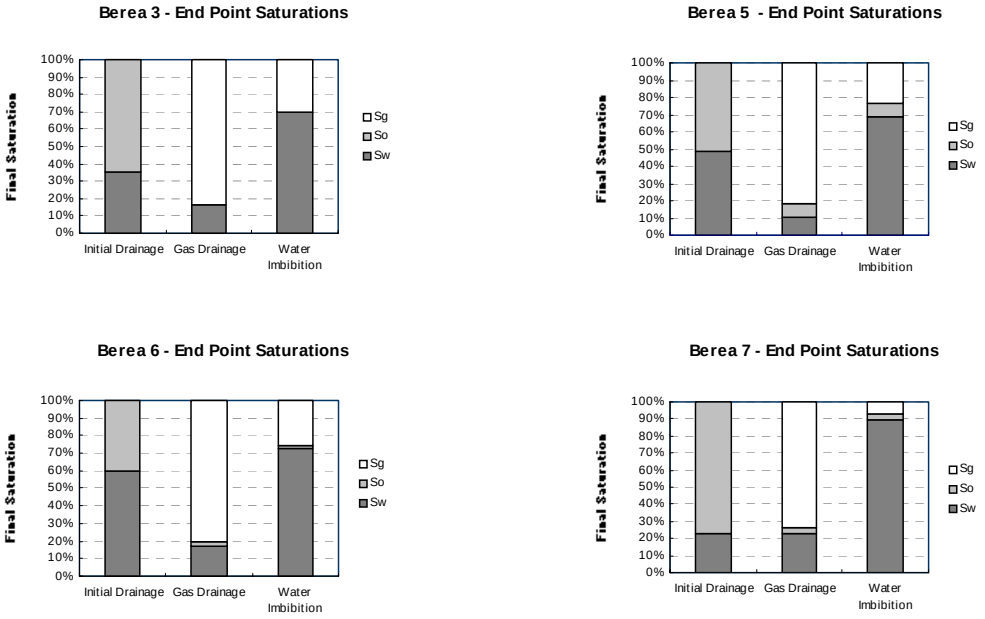

Figure 3: Residual saturations for the tests at 50 bar.

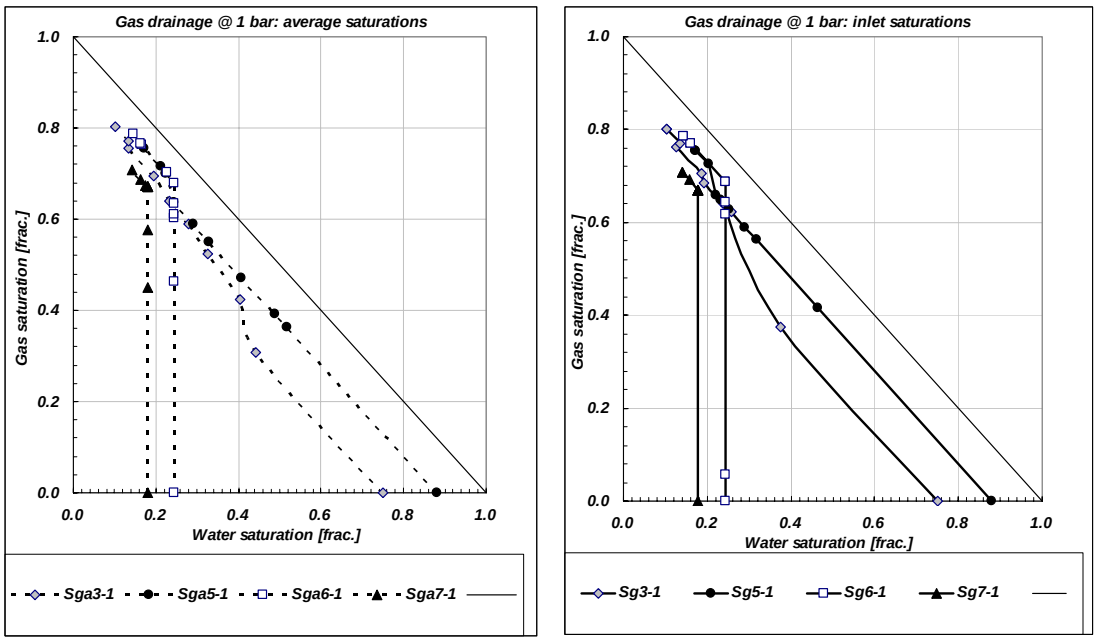

Figure 4: Gas drainage at 1 bar, average (left) and inlet (right) saturation trajectories.

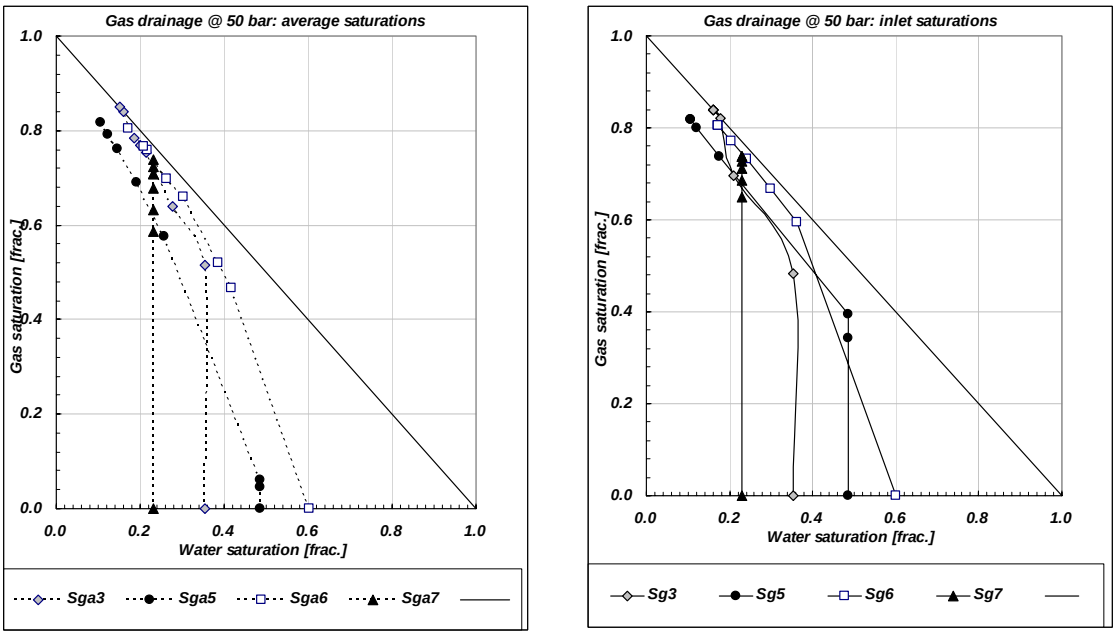

Figure 5: Gas drainage at 50 bar, average (left) and inlet (right) saturation trajectories.

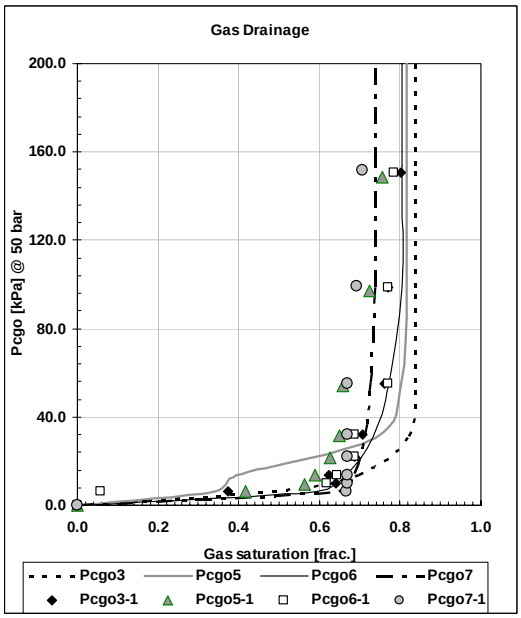

Figure 6: Gas-oil capillary pressures: gas drainage at 1 bar (marks), and 50 bar (curves).

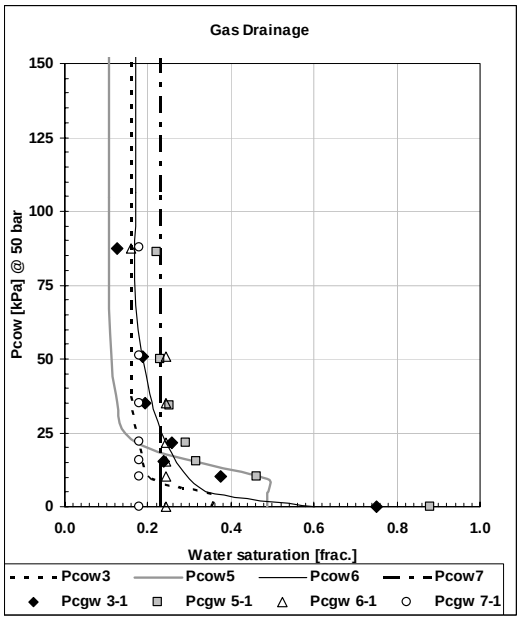

Figure 7: Oil-water capillary pressures: gas drainage at 1 bar (marks), and 50 bar (curves).

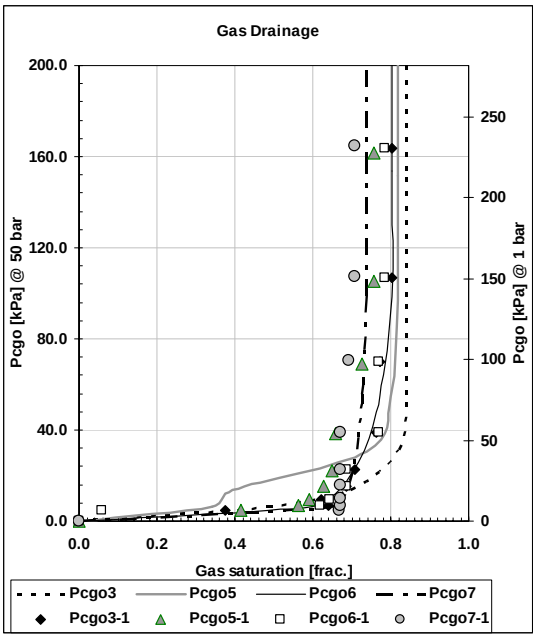

Figure 8: Gas-oil capillary pressures: gas drainage at 1 bar (marks), and 50 bar (solid curves) plotted in different scales.

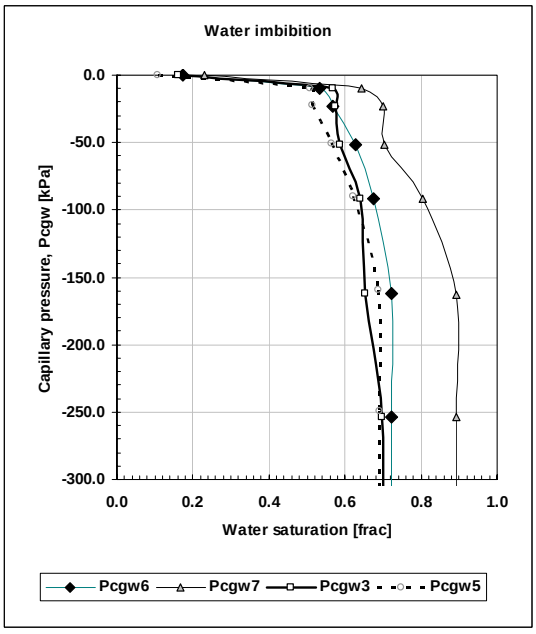

Figure 9: Capillary pressures: water imbibition after gas drainage at 50 bar in the 4 core samples.

TABLE 1: ROTATION RADII OF THE CORE IN CENTRIFUGE		
	Inner radius, cm	Outer radius, cm
Imbibition	14.86	14.86 + L_c
Drainage	15.19 - L_c	15.19

Table 2: Core properties					
		Berea 3	Berea 5	Berea 6	Berea 7
Length	cm	4.78	4.69	4.78	4.81
Diameter	cm	3.78	3.78	3.80	3.79
Porosity	fraction	0.229	0.228	0.227	0.231
Pore volume	cm^3	12.28	11.99	12.32	12.53
Permeability	mD	1148	1184	1206	1184

Table 3: Average saturations, initial and after each displacement at 1 bar								
	Swa3-1	Soa3-1	Swa5-1	Soa5-1	Swa6-1	Soa6-1	Swa7-1	Soa7-1
Initial	1.	0.	1.	0.	1.	0.	1.	0.
Oil drainage	0.751	0.249	0.880	0.120	0.243	0.757	0.179	0.821
Gas drainage	0.103	0.095	0.172	0.072	0.144	0.070	0.141	0.151

Table 4: Average saturations, initial and after each displacement at 50 bar								
	Swa3	Soa3	Swa5	Soa5	Swa6	Soa6	Swa7	Soa7
Initial	1.	0.	1.	0.	1.	0.	1.	0.
Oil drainage	0.354	0.646	0.487	0.513	0.602	0.398	0.230	0.770
Gas drainage	0.150	0.000	0.106	0.077	0.171	0.025	0.230	0.033
Water imbibition	0.698	0.000	0.690	0.077	0.722	0.024	0.894	0.032

Table 5: Brine composition	
SALT	g/l at 20 °C
NaCl	24.7940
Na_2SO_4	4.1400
$NaHCO_3$	0.2070
KCl	0.8010
$MgCl_2*6H_2O$	5.5235
$CaCl_2*2H_2O$	1.2071
$SrCl_2*6H_2O$	0.0125

Table 6: Density of fluids @ 71.1 °C			
P, bar	Brine	Oil (Heptane)	Gas (Methane)
	ρ, g/ml		
1	1.0037	0.6309	0.00174
50	1.0056	0.60939	0.03322
150	1.009	0.53406	0.11349

Table 7: Interfacial tension and spreading				
Pressure, bar	Interfacial Tension, mN/m			Spreading mN/m
	σ_{ow} [1] 23 °C	σ_{gw} [2] 23 °C	σ_{go} 71.1°C	
1	30.6	48.9	14.8	3.5
50	30.6	48.9	10.5	7.8
150	30.6	48.9	3.1	15.2

(1) Interfacial tension between heptane and water (brine) measured with a ring tensiometer at ambient conditions.

(2) Interfacial tension between air and heptane measured with a ring tensiometer at ambient conditions.